Ionic Channels of the Inner Segment of Tiger Salamander Cone Photoreceptors

STEVEN BARNES and BERTIL HILLE

From the Department of Physiology and Biophysics, University of Washington School of Medicine, Seattle, Washington 98195

ABSTRACT Cone photoreceptors were isolated enzymatically and their ionic currents studied by the whole-cell, gigaseal voltage-clamp technique. Five nonsynaptic currents were identified. A prominent, poorly selective cation current, I_h, activated after a delay during hyperpolarizations and then deactivated with a delay on return to potentials > -50 mV. An empirical model for I_h gating kinetics is developed with three open and two closed states. Depolarization elicits a small, voltage-gated calcium current (I_{Ca}). Block by nitrendipine, nickel, cadmium, and cobalt, increase of current with barium, lack of rapid inactivation, and relatively high threshold suggest an L-type Ca channel. No evidence was found for low-threshold Ca channels. An anion current $I_{Cl(Ca)}$ was present after pulses that led to a significant inward I_{Ca} (but not I_{Ba}) and was not elicited when cobalt was present. Tails of $I_{Cl(Ca)}$ were short (100 ms) after short depolarizations and were longer after longer depolarizations. Two TEA-sensitive K currents were also elicited by depolarizations. One, $I_{K(Ca)}$, was calcium sensitive. We looked for modulation of I_h, I_{Ca}, and $I_{Cl(Ca)}$ by a number of neurotransmitters. No changes of I_h were seen, but I_{Ca} and $I_{Cl(Ca)}$ were depressed in a few cones when GABA or adenosine were applied. We discuss how this modulation might contribute to the feedback effects of horizontal cells on cones when surrounding cones are illuminated.

INTRODUCTION

The time course of light responses in vertebrate photoreceptors is determined by interactions between events in the outer and inner segments of the cell. During illumination, electrical responses are initiated by closure of cGMP-sensitive channels of the outer segment, but the resulting photovoltage is shaped significantly by gating of other channels in the inner segment (e.g., Fain and Lisman, 1981). These channels, which may respond to voltage, neurotransmitters, or intracellular free calcium, have been studied extensively in rods, where at least five kinds have been reported. The currents include a nonselective cation current, I_h, activated by hyperpolarization, a voltage-gated calcium current, I_{Ca}, two calcium-activated currents, $I_{Cl(Ca)}$ and $I_{K(Ca)}$, and a voltage-gated and calcium-insensitive I_K (Attwell and Wilson, 1980; Bader et al., 1982; Corey et al., 1984; Hestrin, 1987; Hestrin and Korenbrot, 1987).

Address reprint requests to Dr. Steven Barnes, Dept. of Medical Physiology, University of Calgary, Faculty of Medicine, 3330 Hospital Dr. NW, Calgary, Alberta T2N 4N1 Canada.

J. GEN. PHYSIOL. © The Rockefeller University Press · 0022-1295/89/10/0719/35 $2.00
Volume 94 October 1989 719–743

Our work concerns channels of the inner segment of cones, where less is known. We ask what channels are present and test for effects of neurotransmitters. Evidence has been given for three voltage-gated currents in cones: I_h, I_{Ca}, and $I_{Cl(Ca)}$ (Attwell et al., 1982; Maricq and Korenbrot, 1988). Neurotransmitter-sensitive channels are also expected because, unlike rods, cones receive synaptic "feedback" (Baylor et al., 1971). Indeed channels activated by gamma aminobutyric acid (GABA) and glutamate have been reported in cones (Tachibana and Kaneko, 1984, 1988; Wu, 1986; Kaneko and Tachibana, 1986*a* and *b*; Sarantis et al., 1988). We show that cones have all of the channels that have been described in rods and that some of their currents can be modulated by neurotransmitters. Our results have been reported to the Biophysical Society (Barnes and Hille, 1988).

METHODS

Isolation of Cones

Larval tiger salamanders, *Ambystoma tigrinum* (Kons Scientific Supply, Germantown, WI), were kept at 10°C in an incubator with an 8-h light cycle. For 1–3 d before use, they were

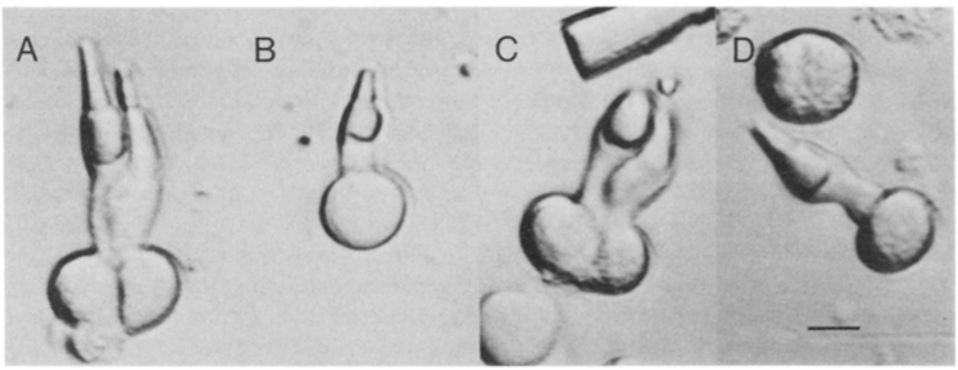

FIGURE 1. Single and double cones isolated from tiger salamander retina. Mechanically isolated cones: (*A*) Principal member (*left*) of double cone had capacitance of 37.3 pF, accessory member (*right*) had 31.0 pF. (*B*) Single cone had 25.7 pF. Enzymatically isolated cones: (*C*) Principal member (*left*) had 12.9 pF, accessory not measured. (*D*) Single cone had 11.3 pF. Scale bar, 10 μm.

kept in a cool tank (17–20°C) with ambient illumination. Animals were killed by decapitation and the head hemisected. Usually the retina was pulled from the eyecup after removal of the cornea and lens within a few minutes of enucleation, but sometimes the intact eyeball was stored for several hours in Ringer's in darkness at 2°C before the retina was removed. Isolated retinas were incubated at 28°C for 15–45 min in 0.5 mg/ml papain (type IV; Sigma Chemical Co, St. Louis, MO) dissolved in standard bath solution. Then they were rinsed for several minutes in enzyme-free Ringer's solution, triturated gently with a cut-off, fire-polished Pasteur pipette, and the cells plated in 200–500-μl wells formed with Sylgard 182 (Dow Corning, Midland, MI) in 35-mm plastic Petri dishes. Dishes with cells survived best in the cold and could be stored up to 6 h at 2°C. Recordings were made at room temperature (21–25°C) from both single and double cones (Fig. 1). During an experiment, the dish of cells sat on the microscope in constant bright illumination from the microscope illuminator.

In most experiments, the cones were isolated after enzyme treatment, as just described, but in a few cases specified in the text, recordings were made from cones isolated by mechanical agitation alone. In these cases, the retina was cut into small pieces in Ringer's solution, drawn several times in and out of a cut-off, fire-polished Pasteur pipette, and the suspension allowed to settle onto the dishes described above. Cells isolated in this manner generally did not stick down securely to the plastic dishes, but they made high resistance seals with the recording electrode, and remained morphologically and electrically intact for several days when stored at 2°C in Ringer's.

In this paper we use the term inner segment to refer to all parts of the cone except the outer segment, and we assume that the channels we study are in the inner segment primarily because Baylor and Nunn (1986) have reported that rod outer segments have <20 pS of residual conductance after the cyclic GMP-activated channels have been closed by a bright light (but see Sather et al., 1985, and Hestrin and Korenbrot, 1987). Some of the cones we studied clearly had lost their outer segments yet they still had voltage- and Ca-activated channels.

Solutions

The NaCl Ringer's solution contained 90 mM NaCl, 2.5 mM KCl, 3 mM $CaCl_2$, 8 mM glucose, 10 mM Hepes, titrated to pH 7.4 with NaOH (Bader and Bertrand, 1984). In many experiements 30 mM of the NaCl was replaced by 30 mM tetraethylammonium (TEA) bromide to reduce currents in K channels. In a few experiments the 3 mM $CaCl_2$ was increased to 10 mM $CaCl_2$, or replaced by 3 or 10 mM $BaCl_2$. Other changes are described in the text or figure legends. One whole-cell pipette solution, called the Cs pipette solution, contained 100 mM CsCl, 2 mM $MgCl_2$, 1 mM EGTA, 100 μM Na_4 guanosine 5'-triphosphate (GTP), 1.5 mM Na_3 ATP, 100 μM leupeptin, 5 mm Hepes, titrated to pH 7.2 with CsOH. Another pipette solution, called Na-K pipette solution, replaced the 100 mM CsCl with 50 mM NaCl and 50 mM KCl (Bader and Bertrand, 1984) and was titrated with KOH to pH 7.2. In a few cases the 1 mM EGTA was replaced by 5 mM 1,2-bis(2-aminophenoxy)ethane *N,N,N',N'*-tetraacetic acid (BAPTA). Leupeptin, ATP, EGTA, and Hepes were obtained from Sigma Chemical Co., GTP from P-L Biochemicals Inc., Milwaukee, WI, BAPTA from Molecular Probes Inc., Eugene, OR, nitrendipine from Miles Pharmaceuticals, West Haven, CT, and Li_4 guanosine-5'-O-(3-thiotriphosphate) (GTPγS) from Boehringer Mannheim Biochemicals, Indianapolis, IN.

Whole-Cell Recording and Analysis

Whole-cell pipettes were pulled from glass hematocrit tubes (VWR Scientific Division, Seattle, WA) in two steps on a vertical pipette puller, coated with Sylgard to within 100 μm of the tip, and lightly fire polished. When filled with intracellular solutions their tip resistances measured in the bath were between 4 and 10 Mohm. Seal resistances ranged from 1 to 20 Gohm. Cones were usually held near a membrane potential of -40 mV, which is close to their normal dark resting potential (Attwell et al., 1982). This potential is also close to the resting potential we measure on these isolated cones in the light with the NaCl Riner's outside and the Na-K pipette solution inside (-39 ± 17 mV, $n = 17$, SD). The membrane current was measured with a List EPC-7 Patch Clamp (Medical Systems Corp., Greenvale, NY) using pipette capacitance compensation but often without whole-cell capacitance or series-resistance compensation. The signal was usually low-pass filtered at 250 Hz (-3 dB point, four-pole Bessel), recorded and stored digitally at 500 Hz (12-bit resolution) with the BASIC-FASTLAB System (Indec Systems, Sunnyvale, CA) incorporating a LabMaster A/D board (Scientific Solutions, Solon, OH) in an IBM AT computer (IBM, Boca Raton, FL). The

BASIC-FASTLAB System also generated the voltage-clamp command stimuli and provided the programs for analysis of data and drawing of figures.

In some of the analysis we attempted to separate components of current by subtracting an appropriate current trace from the record of interest. As is indicated in the figure legends or text, these subtraction traces may have been recorded at the same potential after addition of a blocking drug or may be scaled up from potentials where primarily passive responses are seen. Sometimes the actual trace was used for subtraction, and sometimes an idealized version had to be used to avoid propagation of excess noise.

Membrane capacitance was determined from current records taken with higher frequency response. Small depolarizing voltage steps were applied to the membrane, and the current signal was low-pass filtered at 2.5 kHz and sampled digitally at 50 kHz. The area under the transient portion of the current was used to determine membrane capacitance. In round cells such records can also be used to determine the effective series resistance R_s of the pipette. Taking the early peak amplitude of the recorded transient as an inverse measure of R_s gave high values ranging from 20 to 40 Mohm. These R_s values are likely to be somewhat overestimated, however, because the current transient is attenuated by our filter and the lamellar structure of cone outer segment membranes itself acts like a cable with series resistance to a large, distributed capacitance. According to Attwell et al. (1982), 78% of the surface area of a cone is in the outer segment. If the channels described in this paper are all located on the inner segment membrane, a cable problem in the outer segment will not interfere with our measurements.

Pipette and bath electrode tip potentials were measured against a model 29402 ceramic junction saturated KCl, reference electrode (Beckman Instruments, Inc., Fullerton, CA). For all experiments, recorded whole-cell membrane potentials were corrected by subtracting the appropriate values (between 1 and 12.7 mV).

Bath perfusion was accomplished by gravity-driven inflow via a six-way valve. The bath volume was maintained between 200 and 500 μl by a height-adjustable U-shaped tube connected to a suction pump that allowed rapid (time scale: seconds) bath applications and smooth, nonpulsatile exhaust of media. The neurotransmitter applications of Fig 12 *A* were accomplished with this system. All agents were dissolved at the specified concentration in the appropriate bath solution. The epinephrine and dopamine solutions contained 1 μM dithiothreitol or 10 μM sodium bisulphite to reduce oxidation. Another means of applying neurotransmitters, used for the experiment of Fig. 12 *B*, was a microperfusion pipette driven by an air pressure pulse generator (Pneumatic Picopump, World Precision Instruments, Inc., New Haven, CT) that could be controlled by a digital output of the Indec Systems IBX box. Microejections were made from pipettes having a resistance of 20–50 Mohm when filled with Na-K pipette solution, by 100-ms to 10-s pulses of 10–30 psi nitrogen gas. For making ejections, agents were dissolved in appropriate bath solution.

RESULTS

Passive Properties of Enzyme-treated, Isolated Cones

Seals of >10 Gohm resistance were routinely formed on wider parts of the inner segment. The apparent input resistance fell to 0.5–2 Gohm when breakthrough to the whole-cell configuration was achieved, and a significant slow capacity transient appeared in response to voltage steps. Membrane capacitance was measured on many enzymatically isolated cones by integrating this transient current. It varied from 7 to 62 pF, with a mean of 20 pF (Fig. 2 *A*), suggesting that the isolated cones had a wide range of effective membrane areas. These values were within 3% of the

values obtained in 15 of these cells by using the calibrated capacity compensation dial of the List amplifier. The passive properties were not correlated with whether the cell was a single cone or a double cone. Isolated single and double cones in a random sample had the same capacitance, 23 ± 12 pF (n = 45) and 23 ± 10 pF (n = 18), respectively (mean ± SD). In salamander, double cones are not electrically coupled (Attwell et al., 1984). A previous study reported the membrane capacity of four mechanically isolated tiger salamander cones to be higher (84–100 pF) and more uniform, rationalizing the values obtained in terms of a geometrical model of the membrane infoldings of the outer segment (Attwell, et al., 1982). Therefore we measured a few mechanically isolated cones as well. On average they had higher membrane capacitances (31 pF) than the enzymatically isolated ones (Fig. 2 *B*), suggesting that a variable fraction of the outer-segment surface can be lost during the enzymatic isolation that we use. Even so, the capacitances of our mechanically isolated cones were never as high as those seen by Attwell et al. (1982). When viewed under crossed polarizers, our enzymatically isolated cones showed much less birefringence than the mechanically isolated ones even though, without the polarizers, the outer segments looked normal (compare Fig. 1, *B* and *D*, for example).

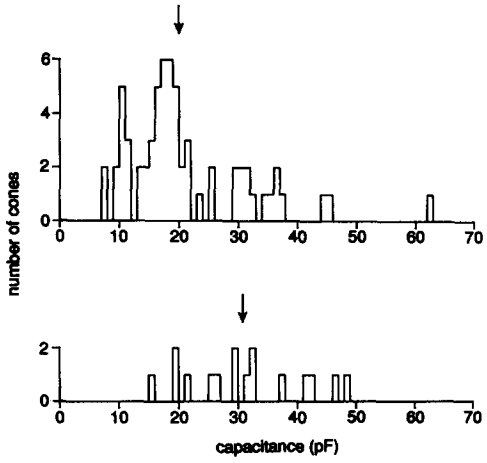

FIGURE 2. Histogram of the input capacitances of cones. (*Upper*) 64 enzymatically isolated cones having a mean capacitance (*arrow*) of 20 ± 10 pF. (*Lower*) 16 mechanically isolated cones having a mean capacitance of 31 ± 10 pF (*arrow*).

Whole-Cell Currents

In all cones, voltage steps away from the holding potential elicited a capacity transient followed by obvious, time-dependent changes of current (Fig. 3). Large depolarizations elicited growing outward currents, large hyperpolarizations elicited growing inward currents, and after pulses in either direction, a tail of inward current appeared. We now consider how these total currents can be dissected into individual components. We identify at least five underlying components.

I_h, an Inward Current Activated by Hyperpolarization

Hyperpolarizing voltage steps from −41 mV elicit a large, slowly developing inward current, I_h, during the pulse and a small, slowly decaying inward tail current at −41

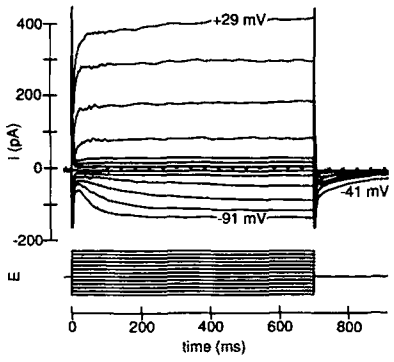

FIGURE 3. Whole-cell voltage clamp currents of a cone. The membrane potential was held at −41 mV and stepped for 700 ms to levels ranging from −91 to +29 mV in 10-mV steps (0.33 Hz). The illuminated, single cone had a resting potential of −33 mV, an input capacity of 34 pF, and an input resistance of 0.9 Gohm (near −41 mV). No series resistance compensation or leak or capacity correction have been used but the capacity transients have been clipped. The pipette contained the Na-K pipette solution and the bath contained NaCl Ringer's solution. If not otherwise noted, all records in the figures were filtered at 250 Hz and sampled at 500 Hz. T = 24°C.

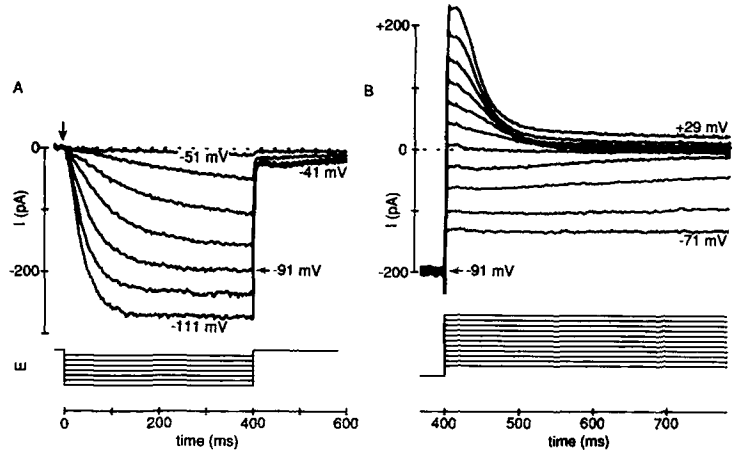

FIGURE 4. I_h in a voltage-clamped principle member of a double cone. (*A*) Activation of I_h by hyperpolarizing steps. The membrane was held at −41 mV and hyperpolarized for 400 ms to potentials ranging from −51 to −111 mV in 10-mV steps. Arrow marks the beginning of the pulse. (*B*) Deactivation of I_h at various membrane potentials. The membrane was hyperpolarized to −91 mV for 400 ms to activate I_h and then returned to potentials ranging from −71 to +29 mV in 10-mV increments. Only the last 30 ms of the hyperpolarization is shown but the full time course of the I_h response was almost identical to that in the −91-mV trace in *A*, and the time axis is labeled the same way. Both panels are from the same cell bathed in a solution containing 30 mM TEA and 6 mM Co^{2+}. The pipette contained the Na-K solution. Test pulses were applied every 3 s. Leak and capacity currents were removed digitally by subtracting a scaled version of the current recorded in a step from −41 to −11 mV.

mV after the pulse (Figs. 3 and 4 *A*). The membrane conductance increases during the hyperpolarization and falls again afterward. I_h was best studied when currents in K channels, Ca channels and calcium-activated channels were reduced by including 30 mM TEA and 6 mM Co^{2+} in the bath solution, as was done in the experiment of Fig. 4. We usually used the Na-K pipette solution to study I_h.

The reversal potential for I_h can be determined from tail currents by activating the conductance at −91 mV and then stepping back to various potentials (Fig. 4 *B*). At all potentials up to −41 mV the tail current is inward, and at −21 mV it is clearly outward, with an interpolated reversal potential E_r = −32.5 mV for the leak-subtracted records in Fig. 4 *B*. This is consistent with previous work in cones and other

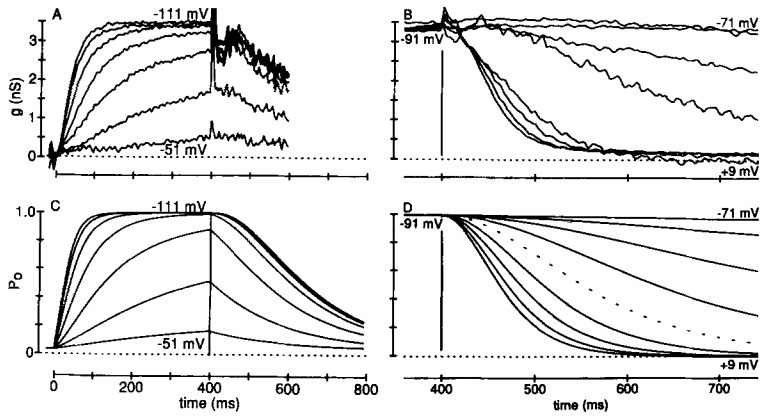

FIGURE 5. Recorded and simulated time courses of the hyperpolarization-activated conductance, g_h. (*A* and *B*) Experimental time courses of g_h calculated from the records of Fig. 4 by the formula, $g_h = I_h/(E - E_r)$, where E is the membrane potential and E_r = −32.5 mV. The records were then smoothed by a digital filter to reduce the frequency response to 125 Hz. (*C* and *D*) Theoretical time courses for the same voltage protocols as in *A* and *B* using the five-state kinetic model outlined in the text. The voltage-dependent rate constants in units of seconds^{-1} were $\alpha = 18/\{\exp[(E + 88)/12] + 1\}$ and $\beta = 18/\{\exp[-(E + 18)/19] + 1\}$. In the formulas E is in millivolts. Because of the assumption of identity of gating particles, the calculations required only solving a single first-order equation for a single gating particle. If p is the probability that this gating particle is in the open position, the fraction of pores open, P_o, equals the probability that at least two of four particles is in the open position, or $1 - (1 + 3p)(1 - p)^3$.

cells (see Discussion) which shows that I_h is a nonselective cation current with a small preference for K^+ ions over Na^+ ions.

The currents of Fig. 4 were converted to ionic conductances by dividing by the electrical driving force, $E - E_r$, where E is the membrane potential and E_r = −32.5 mV (Fig. 5, *A* and *B*). If one neglects capacity current artifacts, the calculated conductances show enough continuity between the end of the test pulse and the beginning of the tail to permit using ohmic conductance as an approximate measure of the number of open channels in these ionic conditions. The midpoint for activation of the conductance and the voltage at which conductance changes are the slowest

both fall between −51 and −61 mV. Activation is greatly speeded with increasing hyperpolarization between −61 and −91 mV (Fig. 5 *A*) and deactivation is greatly speeded with increasing depolarization between −51 and −21 mV (Fig. 5 *B*). The tail conductance at −31 mV is omitted from Fig. 5 *B* because that current is recorded almost at the reversal potential and the calculation is not meaningful, and the conductances at +19 and +29 mV are not drawn because the final decay of I_h there is clearly contaminated with some additional component of outward current. As is common for voltage-gated channels, this one activates with an S-shaped time course (Fig. 5 *A*), which suggests that the channel passes through several closed states before opening. However I_h also deactivates along an S-shaped time course at all potentials between −51 and +9 mV (Fig. 5 *B*), which suggests that the channel passes through several open states before closing. The delay in closing is particularly clear in the large outward currents measured between −11 and +29 mV (Fig. 4 *B*). The delays in activation and deactivation could not be eliminated by adding or removing compensation for the series resistance of the pipette.

Because I_h of vertebrate photoreceptors is known to shape the photoresponse (Fain et al., 1978), it seemed worthwhile to give these currents an empirical quantitative description. We have approximated our observations by a simple kinetic model of the type introduced by Hodgkin and Huxley (1952) and assume that the currents come from a single, homogeneous population of channels. We assume a five-state, linear model with two closed and three open states whose transitions are governed by voltage-dependent rate constants.

$$\mathrm{C} \underset{\beta}{\overset{4\alpha}{\rightleftharpoons}} \mathrm{C} \underset{2\beta}{\overset{3\alpha}{\rightleftharpoons}} \mathrm{O} \underset{3\beta}{\overset{2\alpha}{\rightleftharpoons}} \mathrm{O} \underset{4\beta}{\overset{\alpha}{\rightleftharpoons}} \mathrm{O}$$

The sequence of rate constants is equivalent to having four independent "gating particles," making transitions to their open and closed position with rate constants α and β, respectively. In this model, having any two particles in the open position would suffice to give an open channel. Using values for α and β predicted by the simple empirical expressions in the legend of Fig. 5 yields the conductance time courses shown in Fig. 5, *C* and *D*. They provide an adequate empirical description of the major features of I_h. The assumed voltage dependence of the steady-state probability of having an open channel and the gating-particle transition time constant τ in the model are shown in Fig. 6. The midpoint of the curve of open probability is at −58 mV.

I_h was a robust current seen in 157 of 163 cones. It remained normal looking when ATP, GTP, and leupeptin were all omitted from the pipette solution ($n = 4$) and when 100 μM GTPγS was added to the pipette solution ($n = 16$). Inward and outward I_h was reversibly blocked by adding 5 mM CsCl to the bath (Fig. 7), whereas 30 mM TEA, 5 mM 4-aminopyridine (4-AP), 6 mM Co^{2+}, and 69 mM Ba^{2+} were ineffective. Intracellular Cs^+ was not an effective blocking agent. Even with 100 mM Cs^+ in the pipette, there was clear inward I_h in the potential range from −100 to −40 mV with a slope conductance of 2.5 ± 0.3 nS (SD, $n = 12$), compared with a slope conductance of 4.9 ± 0.4 nS (SD, $n = 18$) with the Na-K pipette solution. Thus the channel is remarkably asymmetrical with respect to the action of Cs^+.

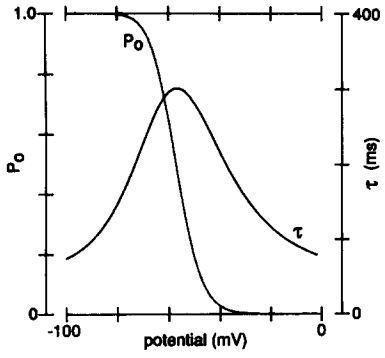

FIGURE 6. Steady-state channel open probability (*left scale*) and gating particle time constant (*right scale*) for the g_h model used in Fig. 4. The time constant τ is $(\alpha + \beta)^{-1}$.

Voltage-gated Ca Channels

A small current in voltage-gated Ca channels could be studied in cones when K currents were reduced by intracellular Cs and extracellular TEA. When a cone was held at −43 mV and depolarized to −3 mV, an inward current developed with a half-time of 2–3 ms and decayed little during the 140-ms depolarization (Fig. 8 *A*). The size of the peak inward current at −3 mV increased 25% when the 3 mM Ca of the external medium was changed to 10 mM Ca, and increased 120% when it was changed to 3 mM Ba (Fig. 8 *A*). The inward current was readily blocked with 10 μM Cd, 20 μM Ni, 1 mM Co, or 10 μM nitrendipine in the bath. The current-voltage relation of I_{Ca} showed clear activation of current beginning with depolarizations to −32 mV (solid and dashed lines, Fig. 8 *B*). The current appears to become outward near +30 mV, a value that is far smaller than the estimated Ca equilibrium potential with out EGTA-containing pipette solutions. This may be partly an artifact of small superimposed outward currents in other channels and partly a consequence of significant outward Cs^+ currents in Ca channels as others have seen (Lee and Tsien, 1984).

The I_{Ca} we have seen has several characteristics of L-type Ca channels (Nowycky et al., 1985): a relatively high threshold, little voltage-dependent inactivation, larger currents in Ba than in Ca, and sensitivity to the dihydropyridine nitrendipine. To look for other possible subtypes of Ca channels, we bathed cones in a Ringer's solu-

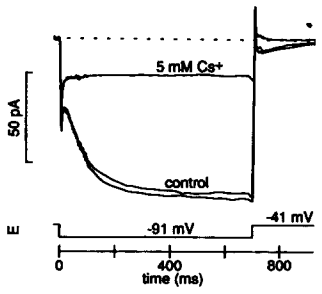

FIGURE 7. Cs^+ block of I_h. I_h is elicited by a 700-ms hyperpolarization from −41 to −91 ms. Traces are taken before, during, and after perfusion of the bath with 5 mM Cs^+ in NaCl Ringer's. The current recorded before Cs is the larger of the two control traces. The pipette contained Na-K pipette solution. Currents are not corrected for leak, but a single point at the peak of the capacity current has been removed.

tion with 5 mM Cs and 30 mM TEA and compared currents obtained with a holding potential of −82 mV with those obtained with −42 mV. There was no evidence for any major additional component of I_{Ca} introduced by holding the membrane at −82 mV. No inward current appeared in the potential range from −62 to −42 mV (Fig. 8 *B*, open and filled circles, and *D*), ruling out a significant contribution of high-threshold Ca channels. At more positive voltages I_{Ca} did decline slightly after its peak.

I_{Ca} was common, although even with our ATP and leupeptin-containing pipette solutions it tended to run down, lasting somewhere between 10 min and 1 h. In 138

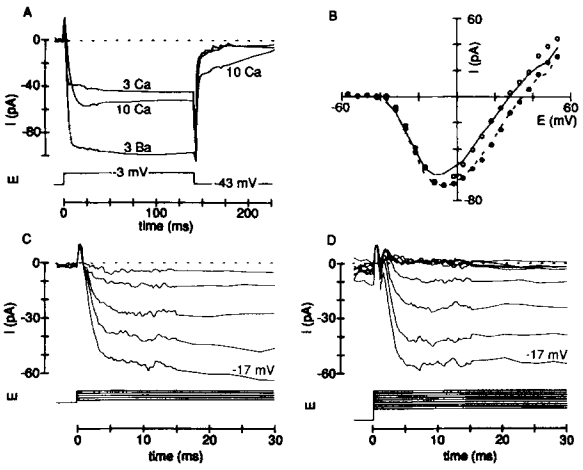

FIGURE 8. Calcium channels in cones. The pipette was filled with the Cs pipette solution, and the bath included 30 mM TEA. (*A*) Leak and capacity-corrected currents measured in 3 and 10 mM Ca, and 3 mM Ba. The single cone was held at −43 mV and stepped to −3 mV for 140 ms. The records in 10 Ca, 3 Ba, and 3 Ca were made at 7, 10, and 12 min, respectively, after going into the whole-cell mode. (*B*) I-V relations for Ca currents in 3 mM Ca measured from holding potentials of −42 mV (*lines*) and −82 mV (*symbols*). Measurements, made from the records in *C* and *D* of this figure, are the mean of the current between 3 and 7 ms (*solid line, open circles*) and between 15 and 30 ms (*dashed line, solid circles*). (*C*) Ca currents measured at −37, −32, −27, −22, and −17 mV with a holding potential of −42 mV in a single cone. The figure was made by subtracting traces fitted to records made after addition of 3 mM Co from records already obtained with 3 mM Ca in the bath. The analogue signal was filtered at 1 kHz and sampled at 4 kHz. For the first 15 ms all points are shown. The remainder are shown averaged in groups of 10 to reduce noise. (*D*) Ca currents measured with the holding potential at −82, stepping to potentials from −57 to −17 mV in 5-mV increments. Subtractions were made as described for *C*.

out of 164 enzymatically dissociated cones tested we either recorded I_{Ca} (or I_{Ba}) directly or inferred its presence from observations of calcium-activated channels to be described below. In a sample of cells where inward current was evident without leak subtraction, the peak I_{Ca} was 34 ± 20 pA (12 cells, 3 mM Ca) and peak I_{Ba} was 138 ± 71 pA (six cells, 10 mM Ba). On the other hand I_{Ca} was present in only one out of five healthy, mechanically dissociated cones tested by the same criteria.

Calcium-activated Anion Channels

We could readily identify two large calcium-activated conductances in isolated cones. Their calcium requirement could be demonstrated by several criteria: activa-

tion by voltage clamp pulses in the potential range where I_{Ca} is large, less activation when the pipette solution contained high concentrations of calcium chelators, and no activation when Ca channels were blocked. We begin with a calcium-activated anion conductance.

The anion current that we will call $I_{Cl(Ca)}$ is seen most readily when currents in K channels are depressed by including 30 mM TEABr in the bath and using the Cs pipette solution. We have usually studied it with 105 mM Cl^- in the pipette and 68.5 mM Cl^- plus 30 mM Br^- in the bath. In these conditions, step depolarizations positive to −30 mV usually evoked a slowly developing conductance increase that decayed slowly upon return to −40 mV and whose reversal potential was near 0 mV. Fig. 9 *A* shows whole-cell currents in response to step depolarizations to −23, +7, and +57 mV measured in 30 mM TEA. The step to −23 evokes an inward

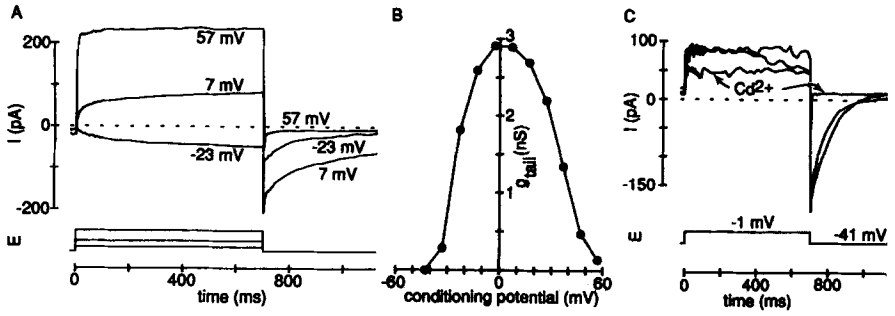

FIGURE 9. Activation of $I_{Cl(Ca)}$ by depolarizing pulses and block by Cd^{2+}. (*A*) Total TEA-insensitive membrane current in response to 700-ms steps to −23, +17, and +57 mV from a holding potential of −43 mV. A single point at the peak of each capacity transient was omitted. (*B*) Tail conductance vs. the voltage of the preceding conditioning pulse potential for the same experiment as *A*. The conductance is calculated from the current 10 ms after the step back to −43 mV using a measured reversal potential $E_{Cl(Ca)}$ of 1 mV. Pulses were applied every 3 s, and the single cone was bathed in a 30-mM TEA bath solution. The whole-cell pipette contained Cs pipette solution. (*C*) Before, during, and after application of 10 μM Cd^{2+} in NaCl Ringer to the bath. The membrane potential is stepped from −41 to −1 mV in a short train of pulses to elicit a large $I_{Cl(Ca)}$ under each condition (as in Fig. 10 *B*). The three traces shown are each the sixth one of the train. The pipette contained Na-K pipette solution.

current that grows slowly throughout the 700-ms pulse, and there is a small inward tail current at −43 mV that takes 300 ms to decay. The step to +7 mV evokes a larger, more rapidly developing outward current and a larger inward tail current at −43 mV. The step to +57 evokes a still larger outward current (most of which is not $I_{Cl(Ca)}$, as described below), followed by almost no tail at −43 mV. In 38 cells responding in this manner, the peak inward tail current flowing near −43 mV after a 700-ms depolarizing pulse to potentials eliciting maximal $I_{Cl(Ca)}$ was 151 ± 121 pA. We focus first on the amplitude of the slow tail current as a measure of the $I_{Cl(Ca)}$ conductance.

Several experiments suggest that the slow tail current at −43 mV requires entry of Ca^{2+} ions through Ca channels during the preceding test pulse. The tail conductance measured 10 ms after the test pulse is plotted against the test-pulse voltage in

Fig. 9 *B*. As we suggested in Fig. 9 *A*, activation of the tail conductance requires some depolarization, is maximal in the voltage range −10 to +10 mV, and is practically nonexistent with large depolarizations to 50 or 60 mV. This voltage dependence presumably reflects a need to depolarize the membrane enough to open L-type Ca channels, while remaining far enough away from the calcium equilibrium potential to have a large Ca^{2+} influx. In other experiments, raising the Ca^{2+} concentration of the bath from 3 to 10 mM increased the size and the duration of the evoked tails (see Fig. 8 *A* for example), and blocking Ca channels with 25 μM Ni^{2+}, 12 μM Cd^{2+}, 1 mM Co^{2+}, or 10 μM nitrendipine reversibly eliminated the evoked slow tail currents (Fig. 9 *C*). Removing the 1 mM EGTA from the pipette solution often made the evoked tails last longer, in a few cases for minutes, and replacing the EGTA with 5 mM BAPTA usually shortened their duraction to tens of milliseconds. Lowering the bath pH to ≤6.8 reversibly eliminated the slow tail current. Like I_{Ca}, the slow tail currents tend to run down with time after whole-cell recording is begun.

Bath-applied caffeine, an agent that releases Ca^{2+} ions from intracellular stores in several other cell types (Endo et al., 1970), turns on a current that probably is $I_{Cl(Ca)}$. When drops containing bath solution supplemented with 1 mM caffeine were applied near the cone under study, a steady inward current appeared near −40 mV that became outward when the cell was depolarized to +20 mV. The current near −40 mV could last for more than 50 s, suggesting that these channels do not always shut quickly at this potential. The quicker decay of tails induced by standard test pulses (Fig. 9 *A*) probably reflects a fast decay of intracellular free calcium after a test pulse rather than an intrinsic gating property that requires the channels to be shut near −40 mV.

There was a clear cumulative effect of depolarizations on the shape of the slow tail current. Isolated, brief test pulses elicited small tail currents that often lasted <100 ms, whereas a test pulse of 1 s or more elicited a tail of quite different shape that took >1 s to decay (Fig. 10 *A*). The longer the test pulse the larger and longer the tail. A similar increase in tail duration occurred if a test pulse of fixed duration was applied several times in succession. The example in Fig. 10 *B* shows a 700-ms test pulse applied every 3 s. When isolated Ca currents were tested with the same pulse paradigm, there was no increase in current magnitude.

If the tail current at −44 mV was due to an electrogenic carrier that is removing Ca^{2+} from the cytoplasm, there would be a stoichiometric relation between the calcium entry during the pulse and the charge carried during the tail. This was not found. The integrals (not shown) of the tail currents in Fig. 10 increase almost exponentially with pulse duration, whereas calcium accumulation should only increase linearly. Furthermore with the 1.43-s test pulse we saw >600 pC of charge in the tail current, whereas the calcium entry (assuming a steady current of 50 pA) probably was only 71 pC. Finally 50 μM ($n = 2$) and 200 μM ($n = 2$) of the Na^{+}-Ca^{2+} exchange inhibitor, dichlorobenzamil, had no effect on the amplitude or time course of the tail current.

A possible explanation of the cumulative effects would consider the time course of relaxation of the excess Ca^{2+} brought into the cell during the test pulse. Suppose the Ca channels are localized near the photoreceptor terminal region and that the

tail current reflects, probably nonlinearly (Evans and Marty, 1986), the time course of the Ca^{2+} concentration near the $I_{Cl(Ca)}$ channels. A short test pulse would cause a localized accumulation of Ca^{2+} at the photoreceptor terminals that would quickly dissipate after the test pulse by local sequestration and diffusion into the rest of the volume of the cell. A long pulse would saturate and fill local sequestering mechanisms and would also permit Ca^{2+} diffusion to spread Ca^{2+} ions throughout the cytoplasm of the cell during the test pulse. Then after the test pulse, no local mech-

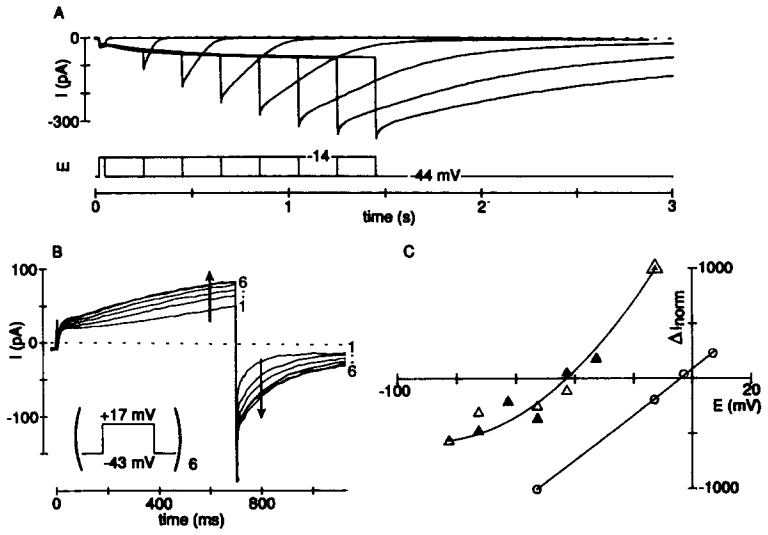

FIGURE 10. Cumulative current increases and the reversal potential for $I_{Cl(Ca)}$. (*A*) Prolongation of slow tail current with longer depolarizing pulses in a single cone. The membrane was stepped at 10-s intervals to −14 mV for durations of 30, 230, 430, 630, 830, 1,030, 1,230, and 1,430 ms from a holding potential of −44 mV. (*B*) Growth of outward current and tail current during repetitive 700-ms depolarizations to +17 mV applied every 3 s. (*C*) Normalized current-voltage relations for $I_{Cl(Ca)}$ with two different pipette solutions and bathed in an all-chloride, Na bath solution. Circles are the Cs pipette solution (104 mM Cl, single cone), and triangles are two cones (single and double) with Cs gluconate pipette solution (14 mM Cl). Currents, ΔI_{norm}, are measured difference currents in the last two digital points before the end of the test pulse from experiments like that in (*B*) and then normalized to arbitrary units using the current measured in fourth and fifth point after the test pulse terminated as described in the text. Currents in *A* and *B* are total membrane current with just one point at the peak of the capacity transient omitted.

anisms would remain for quick reduction of free Ca^{2+}, and instead, slower diffusion into the pipette and export by Na^+-Ca^{2+} exchange and Ca-ATPase would be required to turn off the tail current. The experiments with repetitive pulses (Fig. 10 *B*) show that even when the tail turns off fully in 50–200 ms, there is a residual cumulative effect recognizable 3 s later as a longer tail after the next test pulse. This memory might reflect the inability of overloaded intracellular sequestering mechanisms to empty in 3 s or it might reflect residual phosphorylation or other Ca^{2+}-

induced changes lasting 3 s. Quite probably even the experiment of Fig. 10 *A*, which has a repetition time of 10 s, is contaminated in this way.

Again this explanation of cumulative effects on tail duration suggests that the dominant factor controlling gating of $I_{Cl(Ca)}$ channels in the voltage range from −50 to +50 mV is the intracellular free calcium concentration. However, when the cell was hyperpolarized to −70 or −90 mV the $I_{Cl(Ca)}$ tail decayed faster, as if in this more negative potential range an intrinsic, voltage-dependent gating process may close the channels more rapidly, although this might also be explained by faster Na^+-Ca^{2+} exchange with the hyperpolarization.

What is the reversal potential of this Ca-sensitive current? Because several currents may be activated by the pulse protocol needed to observe $I_{Cl(Ca)}$, we used a subtraction procedure to reduce other contaminating currents. We assumed that $I_{Cl(Ca)}$ is the primary current subject to cumulative activation during trains of depolarizing pulses as in Fig. 10 *B*. Therefore, if the current trace associated with the first pulse of a train is subtracted from those for subsequent pulses, these difference records should reflect $I_{Cl(Ca)}$. One more factor needs to be considered. Trains of pulses delivered at different voltages will not cause the same increment in intracellular free calcium and will not open the same number of Cl(Ca) channels. Fortunately to determine the reversal potential, we are interested in the shape of the current voltage relation but not its amplitude, so the measured currents can be normalized to a constant number of open channels. To generate the difference current-voltage relation shown as open circles in Fig. 10 *C*, trains of test pulses to −13, −3, and +7 mV were delivered to a cone held at −53 mV. Difference currents were measured as described above just before and just after the end of the test pulses. The latter number, the increment in tail amplitude at −53 mV, was used to normalize the former to eliminate variation in the number of channels activated. A quadratic curve fitted to the resulting normalized points passes through zero current at −4 mV, in good agreement with the qualitative reversal potential measurement obtained with the simple pulse protocol of Fig. 9 *A*.

Experiments with various internal and external solutions show that this calcium-activated channel is more permeable to small anions than to small cations and that Cl^- and Br^- are not well distinguished. With the simple pulse protocol of Fig. 9 *A* the reversal potential was the same (near 0 mV) in experiments done with the Cs or the Na-K pipette solutions and when the 30 mM TEA Br in the bath was replaced with TEA Cl, NaCl, or tetramethylammonium bromide or chloride. A preference for anions was suggested by the finding that the slow tail current near −40 mV became larger when the Na^+ and the Cl^- concentrations of the bath solutions were reduced simultaneously. This was done by replacing the 90 mM NaCl either with an isotonic amount of sucrose or with 90 mM NaHepes (pH 7.4) plus sucrose to maintain tonicity. (Note that the 90 mM Hepes buffer contains 40 mM Na^+, 40 mM Hepes anion, and 50 mM Hepes zwitterion.) The anion permeability was demonstrated more clearly by reversal potential measurements done by the cumulative difference method using pipette solutions with a reduced Cl^- concentration. The triangles in Fig. 10 *C* are difference current-voltage measurements made on two cells using a Cs pipette solution where the 100 mM CsCl was replaced with 90 mM Cs gluconate and 10 mM CsCl. The reversal potential was −43 mV, 39 mV more neg-

ative than with the standard Cs pipette solution. If this channel were impermeable to cations and gluconate, the reversal potential should have shifted by 51.2 mV from a predicted +1.4 to −49.8 mV. The smaller size of the observed shift could be accounted for if Cl^- were 14 times more permeable than the alkali metals (Na^+ and K^+) or if Cl^- were 17 times more permeable than gluconate.

Several K Channels

We found evidence for at least two types of K currents activated during depolarizing pulses. One current is probably from high-conductance, calcium-activated K channels and the other may be from calcium-insensitive outwardly rectifying K channels. These currents are seen only with TEA-free bathing solution and with Na-K rather than Cs pipette solutions. To reduce contamination by other currents, we have studied them by subtracting records with 30 mM TEA in the bath from those with the TEA-free solution. We describe them only briefly here.

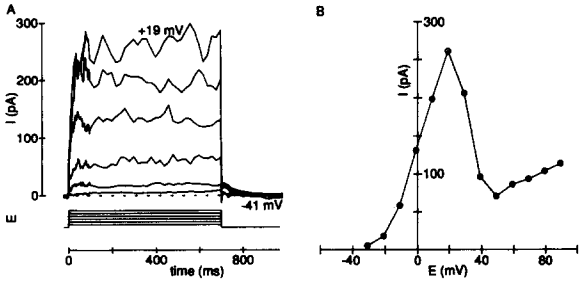

FIGURE 11. Outward currents sensitive to TEA. (*A*) TEA-sensitive currents in response to 700-ms steps to −31, −21, −11, −1, 9, and 19 mV from a holding potential of −41 mV applied at 3-s intervals. The records shown were obtained by digitally subtracting raw data records made in the presence of 30 mM TEA from records made just after the TEA was washed off. The recording pipette contained the Na-K solution. The rising phases were fitted with single exponentials giving time constants of 13 ± 3 ms at −21 mV, 16 ± 6 ms at −11 mV, 11 ± 2 ms at −1 mV, and 19 ± 4 ms at +9 mV. The tail currents decay with an average time constant of 45 ms. (*B*) Current-voltage relation from the cone in *A*. Values plotted are means of the current after digital subtraction during the last 600 ms of the 700-ms depolarizing steps.

The current we will call $I_{K(Ca)}$ is most clearly seen in difference traces (±TEA) measured with depolarizations to between −20 and +20 mV (Fig. 11 *A*). It activates with a half-time of 7–11 ms after the depolarization, does not inactivate during a 700-ms pulse, is very noisy, and gives a small outward tail current decaying with a time constant of ~45 ms at −41 mV. With depolarizations positive to +20 mV, less outward current is elicited, so the current-voltage relation of total TEA-sensitive current is N-shaped (Fig. 11 *B*). In 10 cells having pronounced N-shaped I-V relations the peak noisy outward current was 413 ± 204 pA. Pulses to more positive potentials (+50 to +90 mV) elicit a nearly instantaneous developing outward current that is far less noisy than that at +20 mV. The magnitude of this current was quite variable. The observation that the noisier outward current is maximal at +20 mV suggests that it is activated by Ca^{2+} ions entering through voltage-gated Ca channels. Consistent with this interpretation, the noisy current fails to appear when 1 mM Co is added to the bath. It also is absent in 3 mM Ba Ringer's and is insensitive to 20 mM 4-AP.

The TEA-sensitive current elicited with stronger depolarizations is not reduced by 6 mM Co or by 20 mM 4-AP and is only partly reduced by 3 mM Ba. This current thus does not appear to be calcium activated. We also note that in the presence of 30 mM TEA and 6 mM Co there is a small, instantaneously activated outward current at potentials positive to 0 mV. Even with the Cs pipette solution this small outward current persists. Finally, we have not studied cones using pipette solutions containing high, physiological concentrations of K^+ ions (and no Cs^+ or Na^+ ions), so we cannot rule out the presence of additional K channel types.

Modulation by Neurotransmitters

Because the photoresponses of cones in the intact retina are known to be inhibited by illumination of surrounding cones (Baylor et al., 1971), we looked for possible modulatory actions of neurotransmitters on some of the currents we have described. We tested 80–100 μM concentrations of acetylcholine, muscarine, glutamate, GABA, dopamine, epinephrine, and adenosine. Two of these agents, GABA and glutamate, frequently made conductance increases at all voltages, which we presume represent opening of transmitter-gated channels (Tachibana and Kaneko, 1984 and 1988; Kaneko and Tachibana, 1986*a* and *b*; Sarantis et al., 1988) rather than modulation of voltage-gated channels.

TABLE I

Search for Modulation by Neurotransmitters

Agent	I_h	$I_{Cl(Ca)}$	I_{Ba}
Acetylcholine	0/2	0/4	—
Muscarine	0/1	0/3	—
Glutamate	0/3	0/7	—
GABA	0/4	2/15 (−77%)	1/4 (−77%)
Dopamine	0/3	0/2	—
Epinephrine	0/5	0/4	—
Adenosine	0/2	3/8 (−86%)	—
GABA + adenosine	—	3/10 (−84%)	1/5 (−32%)

The notation "2/15 (−77%)" means, for example, that 2 out of 15 cones tested responded by an average 77% reduction of the measured current.

To look for modulation of I_h, we perfused the bath with each test compound while measuring a full family of I_h relaxations with varying hyperpolarizing steps or while measuring I_h in response to a fixed pulse to −90 mV. The Na-K pipette solution and the 30 mM TEA Ringer's were used. As Table I shows, we found no changes of I_h attributable to any of the compounds tested in a small sample of cells.

To look for modulation of $I_{Cl(Ca)}$, we perfused the bath with test compounds while measuring especially the slow tail current at −43 mV in response to depolarizations to −13 mV. The Cs pipette solution and the 30 mM TEA Ringer's were used. GABA or adenosine reduced $I_{Cl(Ca)}$ reversibly by an average of 83% in eight out of 31 cells, and the other agents had no detected effect on any of the cells (Table I). In some experiments GABA and adenosine were combined in a single solution and the mixture was applied. A typical experiment testing dopamine (DA), glutamate (glu), GABA, and adenosine (ado) is shown in Fig. 12 *A*. Test pulses were given every 3 s

(see insets) and the holding current at −43 mV before the pulse and the tail current at −43 mV after the pulse are plotted. In this cell none of the transmitters effected the holding current, meaning, for example, that this isolated cone has no conventional $GABA_A$ or glutamate-sensitive permeability increase. Furthermore, dopamine, glutamate, and GABA had no effect on the tail current; however, adenosine reduced the $I_{Cl(Ca)}$ tail current strongly and reversibly, and the effect could be repeated.

The modulatory effects of GABA or adenosine on $I_{Cl(Ca)}$ could be indirect, via a

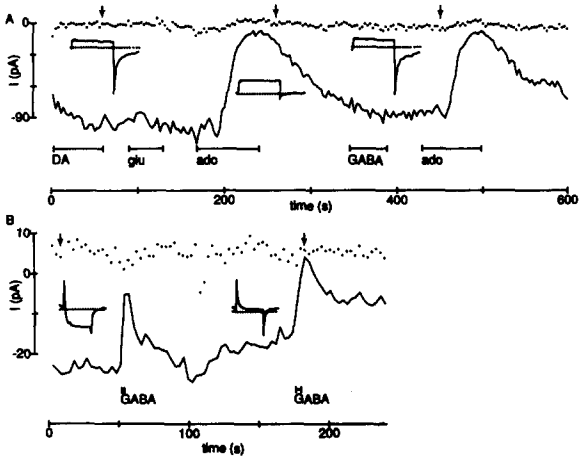

FIGURE 12. Supression of currents in Cl(Ca) and Ca channels. (*A*) Single cone dialyzed with Cs pipette solution was continuously perfused with TEA-containing bath to which 100 μM dopamine, glutamate, adenosine, or GABA had been added. The upper trace (*small symbols*) shows the current required to hold the cell at −43 mV measured just before a 700-ms depolarization to −13 mV applied every 3 s for 10 min. The continuous curve shows the magnitude of each Cl tail current elicited by the depolarizations measured 10 ms after the return to −43 mV. The insets show 800-ms current records at the time of the 20th, 88th, and 151st depolarization (*arrows*). No agent changed the input resistance of the cell at −43 mV, but adenosine was effective at suppressing by 90% the Cl tail current. (*B*) 77% suppression of Ba current by local perfusion with 100 μM GABA of a double cone. The cone, recorded from with a Na-K solution filled pipette, was bath-perfused with a 10 mM Ba and 30 mM TEA solution and stepped from −41 to −11 mV for 70 ms every 3 s. 100 μM GABA, in the same Ba and TEA solution, was driven by a nitrogen pressure pulse of 9 or 12 s duration from a perfusion pipette placed within 200 μm of the cell. The symbols show the holding current at −41 mV just before the voltage step and the continuous line shows the current recorded near the end of the step to −11 mV. The insets show 120-ms records from the third and 60th depolarizations (*arrows*). All points are uncorrected, total membrane current.

reduction of I_{Ca}. To test this possibility, we looked for modulation of barium currents in Ca channels in nine cells (Table I). In two out of nine cells, a reduction of I_{Ba} was seen with GABA (Fig. 12 *B*) or with the GABA plus adenosine mixture. Therefore our working hypothesis is that GABA and adenosine can reduce I_{Ca} in some cones, which produces a secondary change of calcium-sensitive currents such as $I_{Cl(Ca)}$. We have not tested for simultaneous modulation of $I_{K(Ca)}$.

DISCUSSION

We have distinguished at least five nonsynaptic currents in salamander cones: I_h, I_{Ca}, $I_{Cl(Ca)}$, $I_{K(Ca)}$, and a TEA-sensitive, outward current activated by large depolarizations. These are superimposed on currents resulting from background conductances that

we have usually subtracted as a "leak." Similar currents have been described in a variety of rods (Attwell and Wilson, 1980; Bader et al., 1982; Corey et al., 1984; Hestrin, 1987; Hestrin and Korenbrot, 1987), and evidence for I_h has been given in salamander cones (Attwell et al., 1982) and for I_{Ca} and $I_{Cl(Ca)}$ in lizard cones (Maricq and Korenbrot, 1988). Our work is largely consistent with other work. It does not reveal any channels unique to cones. All the channels seem to have a similar counterpart in rods and indeed in a variety of other neurons. One new finding for cones is that I_{Ca} and $I_{Cl(Ca)}$ can in some cases be modulated by GABA and adenosine. No similar modulation has been seen yet in rods, although it is well known in a few other neurons (Holz et al., 1986; Dolphin and Scott, 1987; Scott and Dolphin, 1987).

I_h

Nonselective cation currents activated by hyperpolarization have been described in heart muscle, in one peripheral neuron, and in several central ones, including photoreceptor inner segments, under the various designations I_{AR}, I_f, I_h, and I_Q (and also I_y and I_B). The underlying channel seems approximately the same in each. In most of these cell types it is known to be slightly more permeable to K^+ than to Na^+, blocked by external Cs^+ but not by TEA, half activated at -65 to -90 mV, and characterized by slow gating with time constants between 10 ms and several seconds (Attwell, et al., 1982; Attwell and Wilson, 1980; Bader and Bertrand, 1984; DiFrancesco, 1984; Hestrin, 1987; Mayer and Westbrook, 1983; Spain et al., 1987; Yanagihara and Irisawa, 1980). A lack of block by internal Cs^+ has been noted in cortical neurons (Spain et al., 1987) as we found in cones. The channel may be a multi-ion pore (Hestrin, 1987). It has some resemblance to an inward rectifier, but lacks the high K selectivity, the Ba sensitivity, and the E_K-dependent gating properties of true inward rectifier K channels.

Noisy current records and significant capacity transients have hampered detailed measurements of I_h gating kinetics in neurons. Far better resolution has been achieved in cardiac Purkinje fibers where DiFrancesco (1984) elaborated an eight-state model with three closed states and five open ones. His model gave a very good description when fitted with six free parameters independently at each of 20 test voltages. Our data do not have comparable quality but they suggest for the first time in neurons that multiple open states would be required to explain delays in the closing kinetics. We have described our data approximately at all voltages using a Hodgkin-Huxley–like formalism with six free parameters altogether. This simpler type of model is probably sufficient for good simulation of cone responses even if DiFrancesco's model may more correctly reflect underlying mechanisms. Two clear differences between the I_h kinetics in heart and photoreceptors are that even at 37°C the cardiac channels gate several times slower than the photoreceptor channels at 25°C, and that the midpoint of the gating curve is perhaps 15 mV more negative in heart than in photoreceptors. The I_h current reported in other neurons tends to have an even more negative midpoint than in heart and the faster kinetics of photoreceptors (Mayer and Westbrook, 1983; Spain et al., 1987). In each cell type, the midpoint voltage is near the most negative membrane potential normally achieved by that cell.

In rods I_h becomes activated during the hyperpolarizing response to bright light steps. The resulting inward current shapes the light response by bringing the membrane potential closer to its depolarized dark level even in the presence of continued light (Fain et al., 1978). I_h probably also plays this role in cones, although the extent of shaping is less (Attwell et al., 1983; Attwell, 1986). In heart the size and voltage dependence of I_h are subject to reciprocal modulation by epinephrine and acetylcholine (Tsien, 1974; Brown et al., 1979; DiFrancesco, 1986; DiFrancesco and Tromba, 1987). A similar modulation could have a significant effect on photoresponses in photoreceptors; however, we have thus far not found any (Table I).

I_{Ca}

We and Maricq and Korenbrot (1988) find clear evidence for L-like Ca channels (Nowycky et al., 1985) in enzymatically isolated cones. I_{Ca} may not have been seen in the microelectrode work of Attwell et al. (1982) because it is small and because their mechanical isolation procedure may not preserve it well. We believe that recovery of different anatomical regions of the cone depends on the method of isolation. Enzymatic isolation seems to alter the outer segment, reducing the total cell capacitance, while allowing good preservation of the terminal pedicle (Townes-Anderson et al., 1988) where Ca channels might be preferentially located. Mechanical isolation on the other hand may yield more intact outer segments but may tear off pieces of the pedicle. In addition, several authors (summarized in Hestrin and Korenbrot, 1987) have suggested that enzymatic isolation uncovers latent channels or brings new membrane compartments to the surface of cones (see also Townes-Anderson et al., 1988).

I_{Ca} of cones has an amplitude and voltage dependence similar to that in rods (Bader et al., 1982; Corey et al., 1984; Maricq and Korenbrot, 1988). L-type Ca channels, as defined today, are clearly not identical in all cell types studied, but the properties of I_{Ca} in photoreceptors fall within the range reported in other cells. Among L-type channels, the Ca channels of photoreceptors would be in the group that activates at relatively negative potentials. The midpoint of their activation curve lies near -15 mV, and the maximum inward current is elicited at 0 mV. In chick dorsal root ganglion cells these two numbers are closer to -7 and $+5$ mV (Swandulla and Armstrong, 1988), and in canine atrial cells and clonal pituitary cell they are 0 and 20 mV (Bean, 1985; Matteson and Armstrong, 1986). These values are for physiological levels of extracellular Ca^{2+}.

The voltage-gated Ca channel of photoreceptors may have both electrogenic and messenger functions. The messenger functions could include inhibition of guanylate cyclase (Koch and Stryer, 1988; Rispoli et al., 1988) and stimulation of the release of neurotransmitter from the synaptic terminal when the intracellular free Ca^{2+} concentration ($[Ca^{2+}]_i$) is raised. (Apparently, not all transmitter release from photoreceptors is Ca^{2+} sensitive [Miller and Schwartz, 1983; Schwartz, 1986].) In this role it is appropriate that the activation range of the Ca channel is negative enough so that at least a fraction of these channels would be open at dark resting potentials in the range from -30 to -40 mV, where photoreceptors are tonically releasing transmitter. However, it is apparent that this fraction is very small, so that over most of its operating range between -50 and -30 mV a photoreceptor would have only

a tiny Ca^{2+} entry through voltage-gated Ca channels. This is, however, not the only source of Ca^{2+} influx because the light-sensitive, cation channels of the outer segment also admit a significant Ca^{2+} flux (Nakatani and Yau, 1988). This influx would be shut down by light as well, so that the full story on how $[Ca^{2+}]_i$ is controlled will require a comparison of these two sources while considering the activity of Ca extrusion and buffering mechanisms and the complex geometry of the cone. Thus, for example, the "memory" effects that we saw after calcium loading had been induced by long depolarizations (Fig. 9 *B*) would require a complex explanation.

$I_{Cl(Ca)}$

A chloride conductance activated by intracellular Ca^{2+} was first described in salamander rod photoreceptors and *Xenopus* oocytes (Bader et al., 1982; Miledi, 1982; Barish, 1983). It has subsequently been observed in many neurons and in secretory gland cells. The most complete biophysical analysis, in rat lacrimal gland cells (Evans and Marty, 1986), shows that the channel is broadly permeable to many small anions including NO_3^- and that the probability of opening is increased both by raising $[Ca^{2+}]_i$ and by depolarization. The $[Ca^{2+}]_i$ dependence is steep, suggesting binding of several Ca^{2+} ions to activate the channel, and the voltage dependence is weak, being 10–30 times less steep than for a typical voltage-gated Na, Ca, or K channel. The on- and off-relaxation time constants of the macroscopic current ranged from 70 to 350 ms at 20–25°C when $[Ca^{2+}]_i$ was strongly buffered to constant values. From the more qualitative macroscopic observations in other preparations, except for some authors having reported sensitivity to SITS, we are unaware of any substantiated differences between the calcium-activated anion channels of salamander cones (Maricq and Korenbrot, 1988; and our study), salamander rods (Bader et al., 1982), *Xenopus* oocytes (Miledi, 1982; Barish, 1983), rat dorsal root ganglion cells (Mayer, 1985), mouse spinal neurons (Owen et al., 1986), rat lacrimal gland cells (Evans and Marty, 1986), quail neurons (Bader et al., 1987), and AtT-20 cells (Korn and Weight, 1987).

If the intrinsic voltage dependence of gating of $I_{Cl(Ca)}$ channels in cones is as weak as it is in lacrimal cells, the physiological gating of these channels may simply follow variations in $[Ca^{2+}]_i$. The conductance would be highest in the dark when voltage-gated Ca channels and light-sensitive cation channels are open and lowest in bright light when both are closed. The effect of cone membrane potential would depend on the reversal potential for this primarily anionic current. In our cells the reversal potential is near 0 mV, presumably only because the standard pipette solution has high Cl^-. The in vivo value is not known. The chloride equilibrium potential, E_{Cl}, of cones has variously been estimated to be −46 mV (Miller and Dacheux, 1983) or negative to −50 mV (Kaneko and Tachibana, 1986*a*). As the Ca-activated anion channel is not purely Cl^--selective and may, like many other anion channels, not even be perfectly selective against cations, we will assume that its physiological reversal potential is not as negative as E_{Cl} and is near the dark "resting" potential of the photoreceptor.

Modulation of I_{Ca} and $I_{Cl(Ca)}$

We have found that I_{Ba} or $I_{Cl(Ca)}$ are depressed by GABA or adenosine in 25% of a small sample of enzymatically isolated cones. The simplest hypothesis would be that

the depression of $I_{Cl(Ca)}$ results secondarily from a lowering of $[Ca^{2+}]_i$ when I_{Ca} is depressed. The latter is not without precedent: GABA induces depression of L-type Ca channels in chick DRG neurons (Holz et al., 1986) and adenosine depresses I_{Ca} in rat DRG neurons (Dolphin and Scott, 1987; Scott and Dolphin, 1987). $I_{K(Ca)}$ ought to be depressed as well.

If this kind of modulation were physiologically relevant, what could it do to the light response? In the absence of the modulatory transmitter, a cell in the dark would have a steady, large I_{Ca} and an elevated $[Ca^{2+}]_i$. This would sustain a high rate of photoreceptor transmitter output and an elevated $I_{Cl(Ca)}$. These conditions mean in turn that the photoreceptor is reporting "darkness" to its second-order horizontal and bipolar cells and that the light sensitivity of the photoreceptor is low because of the elevated anion conductance. When modulatory transmitter is present, I_{Ca} is decreased and $I_{Cl(Ca)}$ is decreased. Both conductance decreases may allow the cell to hyperpolarize a bit (even in the dark), which would shut more voltage-gated Ca channels, amplifying the initial modulatory decrease. The net result would be a decreased $[Ca^{2+}]_i$, a decreased photoreceptor transmitter output, and a decreased $I_{Cl(Ca)}$. The photoreceptor would be reporting less "darkness" to its second-order cells even in the dark and this signal would show enhanced light sensitivity due to the lowered input conductance of the cone.

In the retina, cones are subject to lateral inhibition in which illumination of surrounding cones depolarizes a central cone and decreases its light responsiveness (Baylor et al., 1971). This "feedback" results in a membrane conductance increase of the central cone (O'Bryan, 1973; Piccolino and Gerschenfeld, 1980), including perhaps the conductance to Cl^- ions (Lasansky, 1981). In the presence of Ba or Sr, the central cone may even produce a Ba or Sr spike upon surround stimulation (Piccolino and Gerschenfeld, 1978, 1980; Piccolino et al., 1980). The depolarizing action of surround illumination is diminished or even reversed when the central cone is strongly hyperpolarized by a bright spot of light or by injected current (Skrzypek and Werblin, 1983; Attwell et al., 1983).

The feedback effects on a central cone are generally accepted to be mediated by GABA (Ayoub and Lam, 1984) released from horizontal cells. The transmitter should be released tonically from horizontal cells while the surround is dark, and the release would be reduced when the surround is illuminated. Thus feedback would be a cessation of transmitter effect. The feedback effects are usually attributed to Cl conductance changes at the well documented $GABA_A$ receptors found in red and green cones (Murakami et al., 1982; Tachibana and Kaneko, 1984; Kaneko and Tachibana, 1986*a* and *b*). In this $GABA_A$ hypothesis, E_{Cl} is postulated to be more negative than the photoreceptor dark potential so that tonically open $GABA_A$ receptor channels would hyperpolarize the cell, and feedback, by shutting down the Cl conductance, would depolarize the cell. This mechanism gives appropriate potential changes and could reverse at very negative potentials as observed, but by itself, predicts a conductance decrease instead of a conductance increase during feedback. However, conductance increases could result from the depolarization due to activation of voltage- and Ca-gated channels.

Could modulation of I_{Ca} and $I_{Cl(Ca)}$ by GABA, adenosine, and other transmitters in a subset of cones mean that additional mechanisms of feedback exist? Transmitter action on non-$GABA_A$ receptors might have the consequences we deduced earlier in

this subset of cones. A central cone receiving transmitter tonically could have an inhibited I_{Ca}, be somewhat hyperpolarized, and have a higher voltage gain for its light response. Feedback during illumination of the surround could remove the inhibition on I_{Ca}, allow the Cl conductance of the membrane to increase, depolarize the cone, increase the transmitter output, and decrease the voltage gain for its light response. The mechanism would account for depolarization, conductance increases, and "inhibition" during feedback. However, as the modulation mechanism acts through I_{Ca}, it would not account for any feedback effects that can be detected in very hyperpolarized cells where voltage-dependent gating ought to shut Ca channels anyway. Nevertheless, at any potential where these channels let in enough Ca^{2+} to mediate transmitter release onto bipolar and horizontal cells, modulation could change the strength of that signal.

Perhaps a diversity of cone-horizontal cell interactions exists. Only 25% of the cones we tested responded to transmitters with current suppression. The evidence offered by others for $GABA_A$ receptors on red and green cones is extremely strong, as are the effects of $GABA_A$ inhibitors in the intact retina. We can imagine a retinal organization in which the $GABA_A$ system and modulation operate on different subsets of cones or in tandem in the same cone to produce surround inhibition. Our work raises possibilities that now need to be examined pharmacologically in intact retinal preparations (for example, see recent abstracts of Eliasof and Werblin, 1988, and Thoreson and Burkhardt, 1988).

We are grateful to Paul Pfaffinger, Mark Leibowitz, Martha Bosma, Peter Detwiler, Jian Yang, and Laurent Bernheim for helpful discussions throughout this work. We thank Don Anderson and Lea Miller for unfailing technical help.

This work was supported by research grant NS08174 and NRSA training grant NS07097 from the National Institutes of Health and by a McKnight Neuroscience Research Award.

Original version received 3 November 1988 and accepted version received 20 April 1989.

REFERENCES

Attwell, D. 1986. Ion channels and signal processing in the outer retina. *Quarterly Journal of Experimental Physiology.* 71:497–536.

Attwell, D., F. S. Werblin, and M. Wilson. 1982. The properties of single cones isolated from the tiger salamander retina. *Journal of Physiology.* 328:259–283.

Attwell, D., F. S. Werblin, M. Wilson, and S. Wu. 1983. A sign reversing pathway from rods to double and single cones in the retina of the tiger salamander. *Journal of Physiology.* 336:313–333.

Attwell, D., and M. Wilson. 1980. Behavior of the rod network in the tiger salamander retina mediated by properties of individual rods. *Journal of Physiology.* 309:287–315.

Attwell, D., M. Wilson, and S. Wu. 1984. A quantitative analysis of interactions between photoreceptors in the salamander (Ambystoma) retina. *Journal of Physiology.* 352:703–737.

Ayoub, G. S., and D. M. K. Lam. 1984. The release of gamma-aminobutyric acid from horizontal cells of the goldfish (*Carassius auratus*) retina. *Journal of Physiology.* 355:191–214.

Bader, C. R., D. Bertrand, and E. A. Schwartz. 1982. Voltage-activated and calcium-activated currents studied in solitary rod inner segments from the salamander retina. *Journal of Physiology.* 331:253–284.

Bader, C. R., and D. Bertrand. 1984. Effect of changes in intra- and extracellular sodium on the inward (anomalous) rectification in salamander photoreceptors. *Journal of Physiology.* 347:611–631.

Bader, C. R., D. Bertrand, and R. Schlichter. 1987. Calcium-activated chloride current in cultured sensory and parasympathetic quail neurones. *Journal of Physiology.* 394:125–148.

Barish, M. E. 1983. A transient calcium-dependent chloride current in the immature *Xenopus* oocyte. *Journal of Physiology.* 342:309–325.

Barnes, S., and B. Hille. 1988. Ion channels in light-adapted tiger salamander cone photoreceptors. *Biophysical Journal.* 53:390a. (Abstr.)

Barrett, J. N., K. L. Magleby, and B. S. Pallotta. 1982. Properties of single calcium-activated potassium channels in cultured rat muscle. *Journal of Physiology.* 331:211–230.

Baylor, D. A., M. G. F. Fuortes, and P. M. O'Bryan. 1971. Receptive fields of cones in the retina of the turtle. *Journal of Physiology.* 214:265–294.

Baylor, D. A., and B. J. Nunn. 1980. Electrical properties of the light-sensitive conductance of rods of the salamander *Ambystoma tigrinum. Journal of Physiology.* 371:115–145.

Bean, B. P. 1985. Two kinds of calcium channels in canine atrial cells. Differences in kinetics, selectivity, and pharmacology. *Journal of General Physiology.* 86:1–30.

Brown, H., and D. DiFrancesco. 1979. How does adrenaline accelerate the heart? *Nature.* 280:235–236.

Corey, D. P., J. M. Dubinsky, and E. A. Schwartz. 1984. The calcium current in inner segments of rods from the salamander (*Ambystoma tigrinum*) retina. *Journal of Physiology.* 354:557–575.

DiFrancesco, D. 1984. Characterization of the pacemaker current kinetics in calf Purkinje fibres. *Journal of Physiology.* 348:341–367.

DiFrancesco, D. 1986. Characterization of single pacemaker channels in cardiac sino-atrial node cells. *Nature.* 324:470–473.

DiFrancesco, D., and C. Tromba. 1987. Acetylcholine inhibits activation of the cardiac hyperpolarizing-activated current, i_f. *Pflügers Archiv.* 410:139–142.

Dolphin, A. C., and R. H. Scott. 1987. Calcium channel currents and their inhibition by (−)-baclofen in rat sensory neurones: modulation by guanine nucleotides. *Journal of Physiology.* 386:1–17.

Eliasof, S., and F. S. Werblin. 1988. $GABA_B$ modulation of synaptic release from photoreceptors in the tiger salamander. *Investigative Ophthalmology and Visual Science (Supplement).* 29:103.

Endo, M., M. Tanaka, and Y. Ogawa. 1970. Calcium induced release of calcium from the sarcoplasmic reticulum of skinned skeletal muscle fibres. *Nature.* 288:34–36.

Evans, M. G., and A. Marty. 1986. Calcium-dependent chloride currents in isolated cells from rat lacrimal gland. *Journal of Physiology.* 378:437–460.

Fain, G. L., and J. E. Lisman. 1981. Membrane conductances of photoreceptors. *Progress in Biophysics and Molecular Biology.* 37:91–147.

Fain, G. L., F. N. Quandt, B. L. Bastian, and H. M. Gerschenfeld. 1978. Contribution of a caesium-sensitive conductance increase to the rod photoreceptors. *Nature.* 272:467–469.

Hestrin, S. 1987. The properties and function of inward rectification in rod photoreceptors of the tiger salamander. *Journal of Physiology.* 390:319–333.

Hestrin, S., and J. I. Korenbrot. 1987. Voltage-activated potassium channels in the plasma membrane of rod outer segments: a possible effect of enzymatic cell dissociation. *Journal of Neuroscience.* 7:3072–3080.

Hodgkin, A. L., and A. F. Huxley. 1952. A quantitative description of membrane current and its application to conduction and excitation in nerve. *Journal of Physiology.* 117:500–544.

Holz IV, G. G., K. Dunlap, and S. G. Rane. 1986. GTP-binding proteins mediate transmitter inhibition of voltage-dependent calcium channels. *Nature.* 319:670–672.

Kaneko, A., and M. Tachibana. 1986*a*. Effects of γ-amino butyric acid on isolated cone photoreceptors of turtle retina. *Journal of Physiology.* 373:443–461.

Kaneko, A., and M. Tachibana. 1986*b*. Blocking effects of cobalt and related ions on the γ-amino butyric acid-induced current in turtle retinal cones. *Journal of Physiology.* 373:463–479.

Koch, K.-W., and L. Stryer. 1988. Highly cooperative feedback control of retinal rod guanylate cyclase by calcium ions. *Nature.* 334:64–66.

Korn, S. J., and F. F. Weight. 1987. Patch-clamp study of the calcium-dependent chloride current in AtT-20 cells. *Journal of Neurophysiology.* 58:1431–1451.

Lasansky, A. 1981. Synaptic action mediating cone responses to annular illumination in the retina of the larval tiger salamander. *Journal of Physiology.* 310:205–214.

Lee, K. S., and R. W. Tsien. 1984. High selectivity of calcium channels in single dialysed heart cells of the guinea-pig. *Journal of Physiology.* 354:253–272.

Maricq, A. V., and J. I. Korenbrot. 1988. Calcium and calcium-dependent chloride currents generate action potentials in solitary cone photoreceptors. *Neuron.* 1:503–515.

Matteson, D. R., and C. M. Armstrong. 1986. Properties of two types of calcium channels in clonal pituitary cells. *Journal of General Physiology.* 87:161–182.

Mayer, M. L. 1985. A calcium-activated chloride current generates the after-depolarization of rat sensory neurones in culture. *Journal of Physiology.* 364:217–239.

Mayer, M. L., and G. L. Westbrook. 1983. A voltage-clamp analysis of inward (anomalous) rectification in mouse spinal sensory ganglion neurones. *Journal of Physiology.* 340:19–45.

Miledi, R. 1982. A calcium-dependent transient outward current in *Xenopus laevis* oocytes. *Proceedings of the Royal Society B.* 215:491–497.

Miller, A. M., and E. A. Schwartz. 1983. Evidence for the identification of synaptic transmitters released by photoreceptors of the toad retina. *Journal of Physiology.* 334:325–349.

Miller, R. F., and R. F. Dacheux. 1983. Intracellular chloride in retinal neurons: measurement and meaning. *Vision Research.* 23:399–411.

Murakami, M., Y. Shimoda, K. Nakatani, E. Miyachi, and S. Watanabe. 1982. GABA-mediated negative feedback from horizontal cells to cones in carp retina. *Japanese Journal of Physiology.* 32:911–926.

Nakatani, K., and K.-W. Yau. 1988. Calcium and magnesium fluxes across the plasma membrane of the toad rod outer segment. *Journal of Physiology.* 395:695–729.

Nowycky, M. C., A. P. Fox, and R. W. Tsien. 1985. Three types of neuronal calcium channels with different calcium agonist sensitivity. *Nature.* 316:440–443.

O'Bryan, P. M. 1973. Properties of the depolarizing synaptic potential evoked by peripheral illumination in cones of the turtle retina. *Journal of Physiology.* 235:207–223.

Owen, D. G., M. Segal, and J. L. Barker. 1986. Voltage-clamp analysis of a Ca^{2+} and voltage-dependent chloride conductance in cultured mouse spinal neurons. *Journal of Neurophysiology.* 55:1115–1135.

Piccolino, M., and H. M. Gerschenfeld. 1978. Activation of a regenerative calcium conductance in turtle cones by peripheral stimulation. *Proceedings of the Royal Society of London B.* 201:309–315.

Piccolino, M., and H. M. Gerschenfeld. 1980. Characteristics and ionic processes involved in feedback spikes of turtle cones. *Proceedings of the Royal Society of London B.* 206:439–463.

Piccolino, M., J. Neyton, and H. M. Gerschenfeld. 1980. Synaptic mechanisms involved in responses of chromaticity horizontal cells of turtle retina. *Nature.* 284:58–60.

Rispoli, G., W. A. Sather, and P. B. Detwiler. 1988. Effects of triphosphate nucleotides on the response of detached rod outer segments to low external calcium. *Biophysical Journal.* 53:388*a*. (Abstr.)

Sarantis, M., K. Everett, and D. Attwell. 1988. A presynaptic action of glutamate at the cone output synapse. *Nature.* 332:451–453.

Sather, W. A., R. D. Bodoia, and P. B. Detwiler. 1985. Does the plasma membrane of the rod outer segment contain more than one type of ion channel? *Neuroscience Research (Supplement).* 2:S89–S99.

Schwartz, E. A. 1986. Synaptic transmission in amphibian retinae during conditions unfavorable for calcium entry into presynaptic terminals. *Journal of Physiology.* 376:411–428.

Scott, R. H., and A. C. Dolphin. 1987. Inhibition of calcium currents by an adenosine analogue 2-chloroadenosine. *In* Topics and Perspectives in Adenosine Research. E. Gerlach and B. F. Becker, editors. Springer-Verlag, Berlin. 549–558.

Skrzypek, J., and F. S. Werblin. 1983. Lateral interactions in the absence of feedback to cones. *Journal of Neurophysiology.* 49:1007–1017.

Spain, W. J., P. C. Schwindt, and W. E. Crill. 1987. Anomalous rectification in neurons from cat sensorimotor cortex in vitro. *Journal of Neurophysiology.* 57:1555–1576.

Swandulla, D., and C. M. Armstrong. 1988. Fast-deactivating calcium channels in chick sensory neurons. *Journal of General Physiology.* 92:197–218.

Tachibana, M. and A. Kaneko. 1984. γ-aminobutyric acid acts at axon terminals of turtle photoreceptors: Difference in sensitivity among cell types. *Proceedings of the National Academy of Sciences USA* 81:7961–7964.

Tachibana, M. and A. Kaneko. 1988. L-glutamate-induced depolarization in solitary photoreceptors: A process that may contribute to the interaction between photoreceptors in situ. *Proceedings of the National Academy of Sciences, U.S.A.* 85:5315–5319.

Thoreson, W. B. and D. A. Burkhardt. 1988. Cellular mechanisms of surround antagonism in turtle cones. *Society for Neurosciences Abstracts* 14:161.

Townes-Anderson, E., R. F. Dacheux and E. Raviola. 1988. Rod photoreceptors dissociated from the adult rabbit retina. *Journal of Neuroscience.* 8:320–331.

Tsien, R. W. 1974. Effects of epinephrine on the pacemaker potassium current of cardiac Purkinje fibers. *Journal of General Physiology.* 64:239–319.

Wu, S. 1986. Effects of gamma-aminobutyric acid on cones and bipolar cells of the tiger salamander retina. *Brain Research* 365:70–77.

Yanagihara, K. and H. Irisawa. 1980. Inward current activated during hyperpolarization in the rabbit sinoatrial node cell. *Pflügers Archiv.* 385:11–19.